

**NASA
Technical
Paper
3090**

March 1991

**Buckling and Vibration
Analysis of a Simply
Supported Column With
A Piecewise Constant
Cross Section**

Mark S. Lake
and Martin M. Mikulas, Jr.

NASA

Summary

This paper presents an analysis and sample results of the lateral buckling and vibration of a compressively loaded column whose cross section is piecewise constant along its length. The column is symmetric about its midspan and consists of three sections, with the center section having a stiffer cross section than the two identical outboard sections. Buckling and vibration characteristics of the column are determined from a numerical solution of the exact eigenvalue problems. Parametric structural efficiency analyses are performed using a nondimensionalized set of governing equations to determine the optimum ratio between the lengths of the center section and the outboard sections based on both buckling load and vibration frequency requirements. In these analyses two relationships between cross-sectional mass and bending stiffness are considered; one is a low-efficiency method for increasing the bending stiffness of the cross section, and the other is a high-efficiency method. The effect of axial load on vibration frequency is also examined and compared with that of a uniform column.

Introduction

Simply supported columns undergoing lateral vibration and Euler buckling have similar bending-moment distributions with low values near the ends of the column. This suggests that a column with a tapered cross section that is stiffer in the middle than at the ends can be more efficient (i.e., have less mass for a given buckling load) than a uniform column. A buckling analysis of a midspan-symmetric, uniformly tapered column is presented in reference 1, and buckling test results for uniformly tapered columns applicable to large erectable space structures are presented in reference 2. These results have verified the increased structural efficiency of tapered columns compared with uniform columns.

A disadvantage of the continuously tapered column is that it is more difficult to fabricate than a uniform column. The midspan symmetric column with piecewise constant cross section shown in figure 1 is an approximation of a tapered column. This geometry potentially provides some of the increased efficiency of a tapered column without greatly increased fabrication complexity. This paper summarizes the results of a study to quantify the structural efficiency of a midspan symmetric column with a piecewise constant cross section based on both buckling load and vibration frequency considerations. The results derived herein are based on solution of a nondimensionalized set of

governing equations and, therefore are generally applicable to any column of this type.

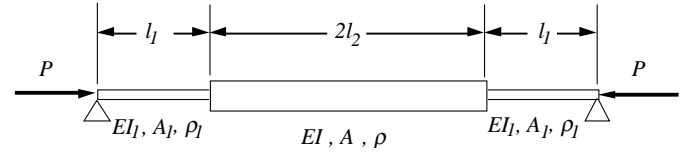


Figure 1. Simply supported column with piecewise constant cross section.

Symbols

A_j	cross-sectional area of j th section
C_{jk}	constants in displacement solution for j th section
$(EI)_j$	flexural stiffness of j th section
l_1	length of outboard sections
l_2	half-length of center section
\bar{M}	normalized mass
P	compressive load
\bar{P}	normalized compressive load
P_{cr}	buckling load
\bar{P}_{cr}	normalized buckling load
r	radius of thin-walled circular cross section
t	time
w_j	lateral displacement of j th section
x, ξ	longitudinal position coordinates
(a)	ratio of length of center section to total column length
β	ratio of flexural stiffness of center section to that of outboard sections
γ	ratio of mass per unit length of center section to that of outboard sections
λ_{jk}	magnitude of k th root of characteristic polynomial for j th section
ρ_j	mass density of j th section
τ	thickness of thin-walled circular cross section
ψ_{jk}	k th root of characteristic polynomial for j th section
ω	vibration frequency

$\bar{\omega}$	normalized vibration frequency
$\bar{\omega}_0$	normalized vibration frequency of column with no axial load

Derivation of Governing Equations

For the present study, it is assumed that the center section of the column shown in figure 1 is of length $2l_2$ with flexural stiffness $(EI)_2$, area A_2 , and density ρ_2 , the outboard sections are each of length l_1 with flexural stiffness $(EI)_1$, area A_1 , and density ρ_1 . Because of symmetry in geometry and loading, it is possible to consider only one-half of the column for analysis. Further, since the fundamental vibration and buckling modes of the column are expected to be symmetric, symmetry boundary conditions are assumed at the column midspan. Figure 2 shows this analysis model along with the assumed boundary conditions.

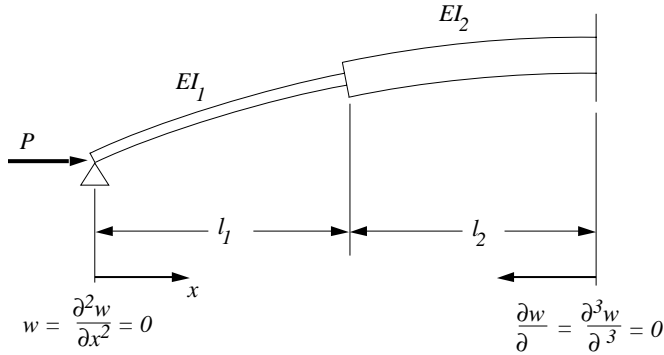


Figure 2. Analysis model.

An exact solution of this problem requires the solution of two fourth-order differential equations, one governing section 1 ($0 \leq x \leq l_1$) and the other governing section 2 ($l_1 \leq x \leq l_1 + l_2$). In addition to the four boundary conditions given in figure 2, four more conditions arise from enforcement of displacement, slope, moment, and shear continuity at the interface between sections 1 and 2 ($x = l_1$). For convenience, a second coordinate axis (ξ) is located with its origin at the column midspan, and the displacement in section 2 is described as a function of this coordinate. The governing differential equation in the j th section is

$$\frac{\partial^4 w_j}{\partial x^4} + \frac{P}{(EI)_j} \frac{\partial^2 w_j}{\partial x^2} + \frac{\rho_j A_j}{(EI)_j} \frac{\partial^2 w_j}{\partial t^2} = 0 \quad (1)$$

The left-end boundary conditions in section 1 are

$$w_1(0) = \frac{\partial^2 w_1}{\partial x^2}(0) = 0 \quad (2)$$

Similarly, the right-end boundary conditions in section 2 are

$$\frac{\partial w_2}{\partial \xi}(0) = \frac{\partial^3 w_2}{\partial \xi^3}(0) = 0 \quad (3)$$

Finally, the continuity conditions between sections 1 and 2 are

$$w_1(l_1) = w_2(l_2) \quad (4)$$

$$\frac{\partial w_1}{\partial x}(l_1) = -\frac{\partial w_2}{\partial \xi}(l_2) \quad (5)$$

$$(EI)_1 \frac{\partial^2 w_1}{\partial x^2}(l_1) = (EI)_2 \frac{\partial^2 w_2}{\partial \xi^2}(l_2) \quad (6)$$

$$(EI)_1 \frac{\partial^3 w_1}{\partial x^3}(l_1) = -(EI)_2 \frac{\partial^3 w_2}{\partial \xi^3}(l_2) \quad (7)$$

Notice that the minus signs exist in equations (5) and (7) because the x and ξ coordinate axes are in opposite directions.

Equation (1) is a homogeneous partial differential equation with constant coefficients. Assuming harmonic motion and applying separation of variables gives the following form for the lateral displacement:

$$w_j(x,t) = C e^{i\omega t} e^{\psi_j x} \quad (8)$$

where C is an arbitrary constant. Substituting equation (8) into equation (1) gives the following characteristic polynomial in ψ_j :

$$\psi_j^4 + \frac{P}{(EI)_j} \psi_j^2 - \frac{\rho_j A_j \omega^2}{(EI)_j} = 0 \quad (9)$$

so that

$$\psi_{j1} = \pm i \sqrt{\frac{P + (P^2 + 4\rho_j A_j (EI)_j \omega^2)^{1/2}}{2(EI)_j}} \quad (10)$$

$$\psi_{j2} = \pm \sqrt{\frac{-P + (P^2 + 4\rho_j A_j (EI)_j \omega^2)^{1/2}}{2(EI)_j}} \quad (11)$$

The right-hand side of equation (10) yields two purely imaginary conjugate roots. The right-hand side of equation (11) yields either a pair of real roots having the same magnitude and opposite signs or, in the static case ($\omega=0$), a pair of repeated roots equal to zero.

Solutions

The equations of the previous section can be solved to determine the critical buckling load of the column by

assuming the vibration frequency to be zero, or they can be solved to determine the fundamental vibration frequency for a fixed value of axial load. First, the solution of the buckling problem will be presented along with numerical examples to assess the structural efficiency of this type of column. Then the solution of the vibration problem will be presented along with similar numerical examples for the case of no applied axial load as well as a range of axial loads.

Solutions for Column Buckling

For $\omega = 0$, $\psi_{12} = \psi_{22} = 0$ and the general solution can be written as follows for the two sections of the column.

$$w_1(x) = C_{11}\sin(\lambda_{11}x) + C_{12}\cos(\lambda_{11}x) + C_{13}x + C_{14} \quad (0 \leq x \leq l_1) \quad (12)$$

$$w_2(\xi) = C_{21}\sin(\lambda_{21}\xi) + C_{22}\cos(\lambda_{21}\xi) + C_{23}\xi + C_{24} \quad (0 \leq \xi \leq l_2) \quad (13)$$

where C_{11} , C_{12} , C_{21} , and C_{22} are arbitrary constants and λ_{11} and λ_{21} are the magnitudes of the roots of the characteristic polynomial ψ_{11} and ψ_{21} given, respectively, by

$$\lambda_{11} = \sqrt{\frac{P}{(EI)_1}} \quad (14a)$$

and

$$\lambda_{21} = \sqrt{\frac{P}{(EI)_2}} \quad (14b)$$

Application of the boundary conditions in equations (2) and (3) reduces the solutions to

$$w_1(x) = C_{11}\sin(\lambda_{11}x) + C_{13}x \quad (0 \leq x \leq l_1) \quad (15)$$

$$w_2(\xi) = C_{22}\cos(\lambda_{21}\xi) + C_{24} \quad (0 \leq \xi \leq l_2) \quad (16)$$

Substituting equations (15) and (16) into the four continuity conditions (equations (4) - (7)) gives the following system of equations for C_{11} , C_{13} , C_{22} , and C_{24} :

$$C_{11}\sin(\lambda_{11}l_1) + C_{13}l_1 = C_{22}\cos(\lambda_{21}l_2) + C_{24} \quad (17)$$

$$C_{11}\lambda_{11}\cos(\lambda_{11}l_1) + C_{13} = C_{22}\lambda_{21}\sin(\lambda_{21}l_2) \quad (18)$$

$$(EI)_1 C_{11}\lambda_{11}^2 \sin(\lambda_{11}l_1) = (EI)_2 C_{22}\lambda_{21}^2 \cos(\lambda_{21}l_2) \quad (19)$$

$$(EI)_1 C_{11}\lambda_{11}^3 \cos(\lambda_{11}l_1) = (EI)_2 C_{22}\lambda_{21}^3 \sin(\lambda_{21}l_2) \quad (20)$$

The existence of a nontrivial solution of equations (17) - (20) requires that

$$\sin(\lambda_{11}l_1) \sin(\lambda_{21}l_2) - \frac{\lambda_{11}}{\lambda} \cos(\lambda_{11}l_1) \cos(\lambda_{21}l_2) = 0 \quad (21)$$

which agrees with the result presented in reference 1. Substituting the definitions for λ_{11} and λ_{21} from equation (14) into equation (21) gives the following transcendental equation for the buckling load, P_{cr} .

$$\sin\left[\frac{P_{cr}l_1^2}{(EI)_1}\right]^{1/2} \sin\left[\frac{P_{cr}l_2^2}{(EI)_2}\right]^{1/2} - \left[\frac{(EI)_2}{(EI)_1}\right]^{1/2} \cos\left[\frac{P_{cr}l_1^2}{(EI)_1}\right]^{1/2} \cos\left[\frac{P_{cr}l_2^2}{(EI)_2}\right]^{1/2} = 0 \quad (22)$$

We now define the dimensionless parameters, α , β , and \bar{P}_{cr} respectively, as follows:

$$\alpha = \frac{l_2}{l_1 + l_2} \quad (23)$$

$$\beta = \frac{(EI)_2}{(EI)_1} \quad (24)$$

$$\bar{P}_{cr} = \frac{P_{cr}}{\pi^2(EI)_1/4(l_1 + l_2)^2} \quad (25)$$

Notice that α is the ratio of the length of the center section to the total column length, β is the ratio of the bending stiffness of the center section to that of the outboard sections, and \bar{P} is the buckling load of the complete column normalized to that of a column having the same length and a uniform bending stiffness equal to that of the outboard sections. Using these nondimensional parameters, equation (22) can be rewritten in the following form.

$$\sin\left[\frac{\pi(1-\alpha)\sqrt{\bar{P}_{cr}}}{2}\right] \sin\left(\frac{\pi\alpha\sqrt{\bar{P}_{cr}}}{2\sqrt{\beta}}\right) - \sqrt{\beta} \cos\left[\frac{\pi(1-\alpha)\sqrt{\bar{P}_{cr}}}{2}\right] \cos\left(\frac{\pi\alpha\sqrt{\bar{P}_{cr}}}{2\sqrt{\beta}}\right) = 0 \quad (26)$$

Numerical Examples and Illustration of Mass Savings

Due to its transcendental form, equation (26), with α and β prescribed, must be solved for \bar{P} numerically. The secant method (ref. 3) is selected due to its simplicity and stable convergence characteristics. To insure the lowest root is found, a search is performed to

determine an initial interval in which the solution exists. During this search, the left-hand side of equation (26) is evaluated for successively larger values of \bar{P} (starting with the lowest possible value, 1.0) until a sign change is detected. The initial solution interval is then bounded by the last two values selected for \bar{P} . Further iteration yields the solution to the desired accuracy.

In order to evaluate the structural efficiency of the column, it is necessary to calculate not only its normalized buckling load but also its normalized mass. For this, two additional dimensionless parameters γ and \bar{M} are defined, respectively, as

$$\gamma = \frac{\rho_2 A_2}{\rho_1 A_1} \quad (27)$$

which is the ratio of mass per unit length in the center section of the column to that of the outboard sections, and

$$\bar{M} = \frac{\rho_1 A_1 l_1 + \rho_2 A_2 l_2}{\rho_1 A_1 (l_1 + l_2)} = 1 + \alpha(\gamma - 1) \quad (28)$$

which is the mass of the column normalized to that of a column having the same total length and a uniform cross section equal to that of the outboard sections.

To illustrate the mass savings possible with this type of column, two different relationships between mass and bending stiffness are considered. The first is a low-efficiency method for increasing the bending stiffness of the cross section; the second is a high-efficiency method. In both cases it is assumed for simplicity that a single material is used throughout the column. In the first case mass and bending stiffness are assumed to be proportional, thus $\gamma = \beta$ in equation (28). To illustrate this case, equations (29) and (30) give the approximate relationships for the area and moment of inertia of a thin walled cylinder, where r is the radius and τ is the thickness:

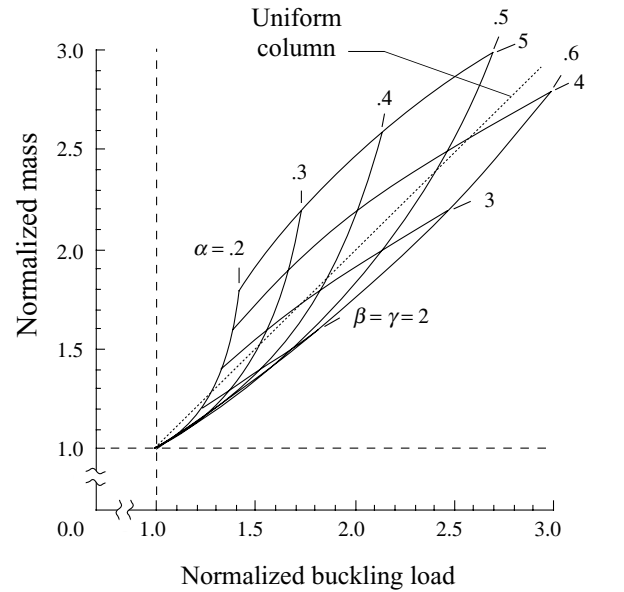
$$\text{Area} \approx 2\pi r\tau \quad (29)$$

$$\text{Moment of inertia} \approx \pi r^3 \tau \quad (30)$$

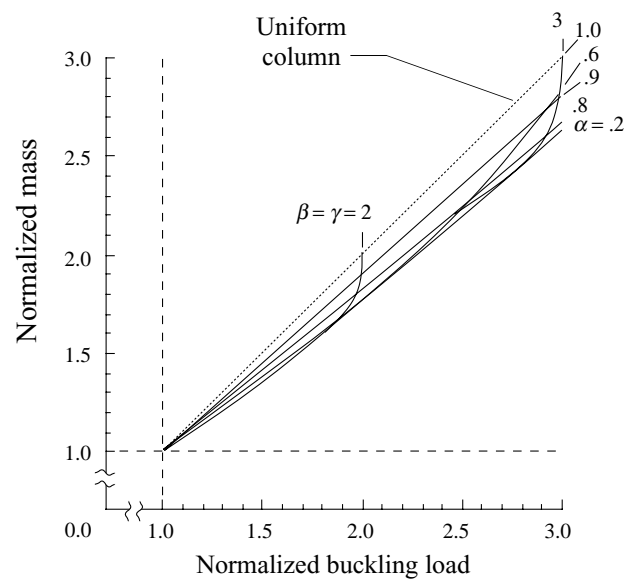
Increasing the thickness while holding the radius constant increases both the area and moment of inertia proportionally, thus $\gamma = \beta$.

Figure 3 presents plots of the normalized column mass versus normalized buckling load determined from equation (26) for an array of length ratios ($0.2 \leq \alpha \leq 0.6$ for fig. 3(a), and $0.6 \leq \alpha \leq 1.0$ for fig. 3(b)) and bending stiffness ratios ($1.0 \leq \beta \leq 6.0$). The dotted-line curves in these figures show the increase in mass necessitated by the increase in buckling load of a uniform column ($\alpha =$

1.0). Therefore, points that lie below these dotted-line curves represent columns that are more efficient (lower in mass) than the uniform column. The data are separated into two parts for clarity. Notice that every curve of constant α is vertically asymptotic to the buckling load of a uniform column with a length $1 - \alpha$ times the length of the original column, i.e., $2l_1$. This is consistent with the fact that when the bending stiffness of the center section is very large, it behaves like a rigid section.



(a) $0.2 \leq \alpha \leq 0.6$.



(b) $0.6 \leq \alpha \leq 1.0$.

Figure 3. Mass versus buckling load where mass is proportional to bending stiffness.

For increases in buckling load up to a factor of 3, it appears that the optimum value for the length ratio α is approximately 0.7 because this corresponds to the lowest curve on the plot. Mass savings is calculated by determining the percent difference between the lowest curve and the uniform column curve ($\alpha = 1.0$) at any given buckling load. It is seen that a mass savings of 10 to 12 percent can be realized by increasing the bending stiffness of the center 70 percent of the column rather than the entire length of the column. Again, this conclusion is based on the assumption that mass and bending stiffness are proportional.

The second relationship considered between mass and bending stiffness, the mass is assumed to be pro-

portional to the cube root of the bending stiffness (i.e. $\gamma = \sqrt[3]{\beta}$ in equation (28)). This case is representative of high-efficiency methods for increasing the bending stiffness of the cross section, and it is illustrated by a thin-walled circular cross section in which the radius is increased while the thickness is held constant (See eqs. (29) and (30).)

Figure 4 presents plots of the normalized column mass versus normalized buckling load for this case. As before, the dotted-line curves in this figure show the increase in mass using a uniform column ($\alpha = 1.0$), and the data points below these curves represent columns that are more efficient (less massive) than the uniform column.

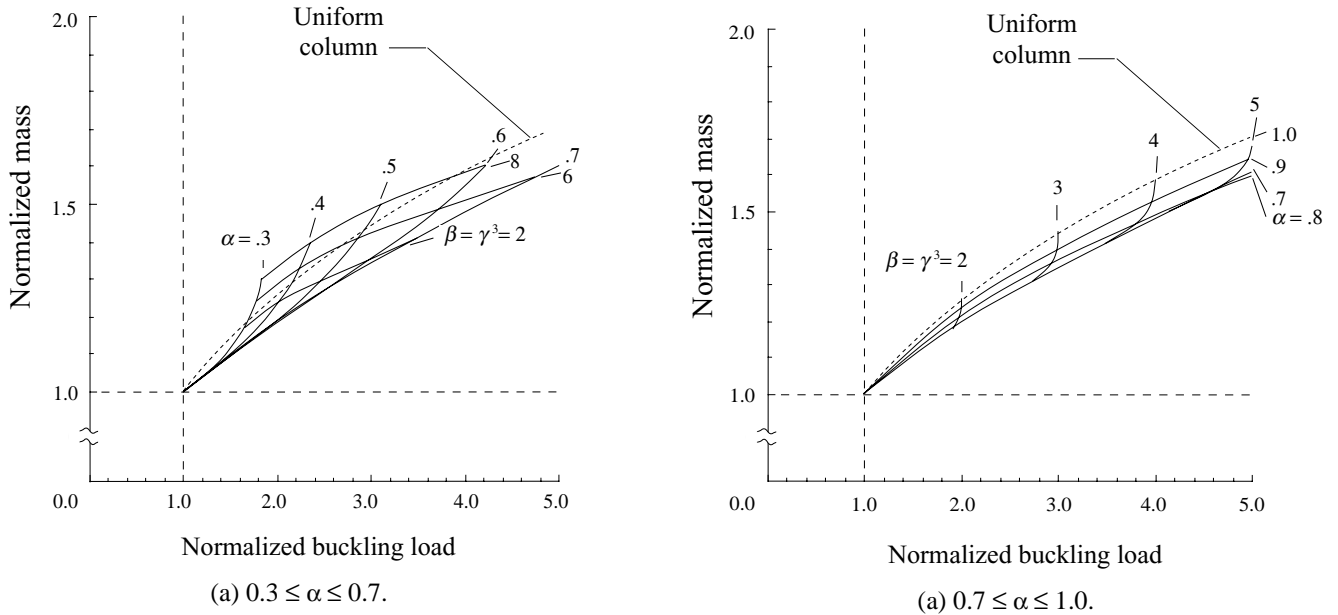


Figure 4 Mass versus buckling load where mass is proportional to the cube root of the bending stiffness.

As was determined in the first case, it appears that the optimum value for the length ratio α is approximately 0.7. In this case a mass savings of about 6 to 8 percent is realized by increasing the bending stiffness of the center 70 percent of the column rather than the entire length of the column. Again, this conclusion is based on the assumption that mass is proportional to the cube root of the bending stiffness.

Solution for Column Vibration

For vibration of the column under a specified axial load P , the general solutions are as follows:

$$w_1(x,t) = e^{i\omega t} [C_{11}\sin(\lambda_{11}x) + C_{12}\cos(\lambda_{11}x) + C_{13}\sinh(\lambda_{12}x) + C_{14}\cosh(\lambda_{12}x)] \quad (0 \leq x \leq l_1) \quad (31)$$

$$w_2(\xi,t) = e^{i\omega t} [C_{21}\sin(\lambda_{21}\xi) + C_{22}\cos(\lambda_{21}\xi) + C_{23}\sinh(\lambda_{22}\xi) + C_{24}\cosh(\lambda_{22}\xi)] \quad (0 \leq \xi \leq l_2) \quad (32)$$

where, as before, C_{11} , C_{12} , C_{21} , C_{22} , C_{13} , C_{23} , C_{14} , and C_{24} are arbitrary constants and λ_{11} , λ_{12} , λ_{21} , and λ_{22} are defined as

$$\lambda_{11} = \sqrt{\frac{P + [P^2 + 4\rho_1 A_1 (EI)_1 \omega^2]^{1/2}}{2(EI)_1}} \quad (33a)$$

$$\lambda_{21} = \sqrt{\frac{P + [P^2 + 4\rho_2 A_2 (EI)_2 \omega^2]^{1/2}}{2(EI)_2}} \quad (33b)$$

$$\lambda_{12} = \sqrt{\frac{-P + [P^2 + 4\rho_1 A_1 (EI)_1 \omega^2]^{1/2}}{2(EI)_1}} \quad (34a)$$

$$\lambda_{22} = \sqrt{\frac{-P + [P^2 + 4\rho_2 A_2 (EI)_2 \omega^2]^{1/2}}{2(EI)_2}} \quad (34b)$$

Upon application of the boundary conditions in equations (2) and (3), the general solutions reduce to

$$w_1(x,t) = e^{i\omega t} [C_{11} \sin(\lambda_{11}x) + C_{13} \sinh(\lambda_{12}x)] \quad (0 \leq x \leq l_1) \quad (35)$$

$$w_2(\xi,t) = e^{i\omega t} [C_{22} \cos(\lambda_{21}\xi) + C_{24} \cosh(\lambda_{22}\xi)] \quad (0 \leq \xi \leq l_2) \quad (36)$$

Substituting equations (35) and (36) into the continuity conditions (eqs. (4)-(7)) gives the following system of equations that are written here in matrix form:

$$\begin{bmatrix} \sin(\lambda_{11}l_1) & \sinh(\lambda_{12}l_1) & -\cos(\lambda_{21}l_2) & -\cosh(\lambda_{22}l_2) \\ \cos(\lambda_{11}l_1) & \frac{\lambda_{12}}{\lambda_{11}} \cosh(\lambda_{12}l_1) & -\frac{\lambda_{21}}{\lambda_{11}} \sin(\lambda_{21}l_2) & \frac{\lambda_{22}}{\lambda_{11}} \sinh(\lambda_{22}l_2) \\ -\sin(\lambda_{11}l_1) & \left(\frac{\lambda_{12}}{\lambda_{11}}\right)^2 \sinh(\lambda_{12}l_1) & \beta \left(\frac{\lambda_{21}}{\lambda_{11}}\right)^2 \cos(\lambda_{21}l_2) & -\beta \left(\frac{\lambda_{22}}{\lambda_{11}}\right)^2 \cosh(\lambda_{22}l_2) \\ -\cos(\lambda_{11}l_1) & \left(\frac{\lambda_{12}}{\lambda_{11}}\right)^3 \cosh(\lambda_{12}l_1) & \beta \left(\frac{\lambda_{21}}{\lambda_{11}}\right)^3 \sin(\lambda_{21}l_2) & \beta \left(\frac{\lambda_{22}}{\lambda_{11}}\right)^3 \sinh(\lambda_{22}l_2) \end{bmatrix} \begin{bmatrix} C_{11} \\ C_{13} \\ C_{22} \\ C_{24} \end{bmatrix} = 0 \quad (37)$$

where β is the bending stiffness ratio defined in equation (24).

As in the case of the buckling problem, it is of interest to nondimensionalize the vibration eigenvalue problem to allow general solution curves to be constructed. In addition to the dimensionless length, bending stiffness, and mass per unit length parameters defined in equations (23) - (25), a dimensionless vibration frequency $\bar{\omega}$ and compressive load \bar{P} are defined, respectively, by

$$\bar{\omega} = \frac{\omega}{\pi^2 \sqrt{\frac{(EI)_1}{16\rho_1 A_1 (l_1 + l_2)^4}}} \quad (38)$$

$$\bar{P} = \frac{P}{\pi^2 (EI)_1 / 4(l_1 + l_2)^2} \quad (39)$$

Hence, the vibration frequency and compressive load are normalized to the fundamental frequency and buckling load, respectively, of a uniform column of the same length with bending stiffness and mass per unit length equal to that of the outboard sections (ref. 4).

All the parameters in equation (37) may now be written in terms of the five dimensionless quantities: α , β , γ , \bar{P} , and $\bar{\omega}$. The resulting expressions are

$$\lambda_{11}l_1 = \frac{\pi(1-\alpha)}{\left[\bar{P} + \left(\bar{P}^2 + \bar{\omega}^2\right)^{1/2}\right]^{1/2}} \quad (40)$$

$$\lambda_{12}l_1 = \frac{\pi(1-\alpha)}{\left[-\bar{P} + \left(\bar{P}^2 + \bar{\omega}^2\right)^{1/2}\right]^{1/2}} \quad (41)$$

$$\lambda_{21}l_2 = \frac{\pi\alpha}{2\sqrt{\beta}} \left[\frac{\bar{P}}{2} + \left(\frac{\bar{P}^2}{4} + \gamma\beta\bar{\omega}^2 \right)^{1/2} \right]^{1/2} \quad (42)$$

$$\lambda_{22}l_2 = \frac{\pi\alpha}{2\sqrt{\beta}} \left[-\frac{\bar{P}}{2} + \left(\frac{\bar{P}^2}{4} + \gamma\beta\bar{\omega}^2 \right)^{1/2} \right]^{1/2} \quad (43)$$

$$\frac{\lambda_{12}}{\lambda_{11}} = \left[\frac{-\frac{\bar{P}}{2} + \left(\frac{\bar{P}^2}{4} + \bar{\omega}^2 \right)^{1/2}}{\bar{P} + \left(\frac{\bar{P}^2}{4} + \bar{\omega}^2 \right)^{1/2}} \right]^{1/2} \quad (44)$$

$$\frac{\lambda_{21}}{\lambda_{11}} = \frac{1}{\sqrt{\beta}} \left[\frac{\frac{\bar{P}}{2} + \left(\frac{\bar{P}^2}{4} + \gamma\beta\bar{\omega}^2 \right)^{1/2}}{\bar{P} + \left(\frac{\bar{P}^2}{4} + \bar{\omega}^2 \right)^{1/2}} \right]^{1/2} \quad (45)$$

$$\frac{\lambda_{22}}{\lambda_{11}} = \frac{1}{\sqrt{\beta}} \left[\frac{-\frac{\bar{P}}{2} + \left(\frac{\bar{P}^2}{4} + \gamma\beta\bar{\omega}^2 \right)^{1/2}}{\bar{P} + \left(\frac{\bar{P}^2}{4} + \bar{\omega}^2 \right)^{1/2}} \right]^{1/2} \quad (46)$$

Numerical Examples for Column Vibration

Equation (37) must be solved numerically to determine the normalized vibration frequency $\bar{\omega}$, given values for the other nondimensional parameters. Again, the secant method was used to determine the lowest value of $\bar{\omega}$ that causes the determinant of the matrix in equation (37) to vanish. The determinant of equation (37) was calculated using a Gaussian elimination procedure presented in reference 5.

Natural vibration of columns without axial load.

In the last section, the structural efficiency of columns with piecewise constant cross sections was quantified based on buckling performance. It is also of interest to determine vibration performance of these columns with no axial load. Consequently, equations (37) and (28) were solved to determine the vibration frequencies and masses for the same array of length ratios ($0.2 \leq \alpha \leq 1.0$) and bending stiffness ratios ($1.0 \leq \beta \leq 6.0$) considered in the buckling solutions. As before, two cases were considered involving the mass per unit length of the cross section. In the first case it was assumed that the mass and bending stiffness of the cross section are proportional (i.e., $\gamma = \beta$). In the second case it was assumed that the mass is

proportional to the cube root of the bending stiffness (i.e., $\gamma = \sqrt[3]{\beta}$).

Figure 5 presents a plot of the normalized column mass versus normalized vibration frequency for the first case ($\gamma = \beta$). It should be noted that for a uniform column ($\alpha = 1.0$), there is no change in the frequency as the bending stiffness and mass are increased proportionately. The significant result determined from figure 5 is that all column geometries considered exhibit frequencies that are lower than the uniform column having the same mass. Therefore, in the case where the distributed mass of the column is proportional to its bending stiffness, a column with piecewise constant cross section is less efficient than a uniform column, based on vibration frequency, in contrast to results based on buckling load.

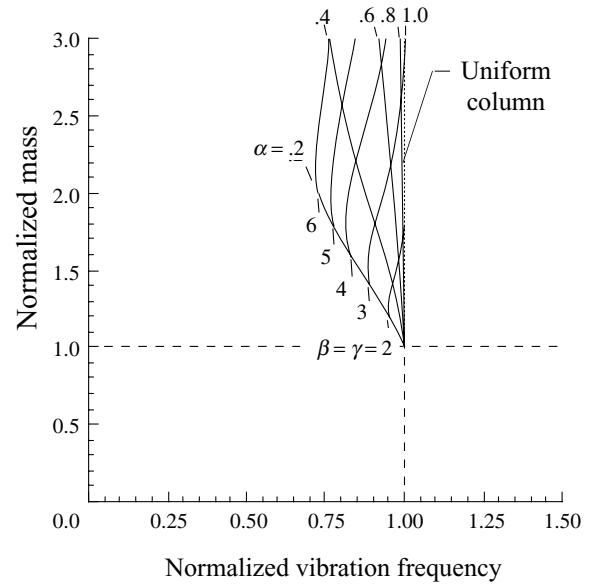


Figure 5. Mass versus vibration frequency where mass is proportional to bending stiffness.

Figure 6 presents plots of the normalized column mass versus normalized vibration frequency for the second case ($\gamma = \sqrt[3]{\beta}$). The dotted lines in these figures show the increase in mass for a uniform column ($\alpha = 1.0$); thus the data points below these lines represent columns that are more efficient than the uniform column based on fundamental vibration frequency. Again, the data are separated into two parts for clarity.

The trends displayed in figure 6 are similar to those presented in figures 3 and 4 and discussed in the buckling analysis of the last section. In this case, the total column mass can be minimized by stiffening the center 70 to 80 percent of the column. Furthermore,

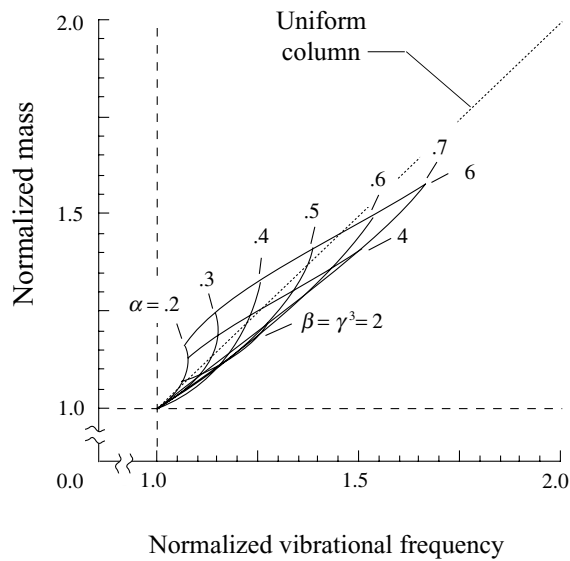
the use of this design results in a mass savings of approximately 10 to 15 percent relative to a uniform column with the same vibration frequency.

Vibration of columns under axial load. The effect of axial load on the fundamental vibration frequency of a uniform column is analyzed in reference 6. The normalized formula for calculating this frequency can be written as

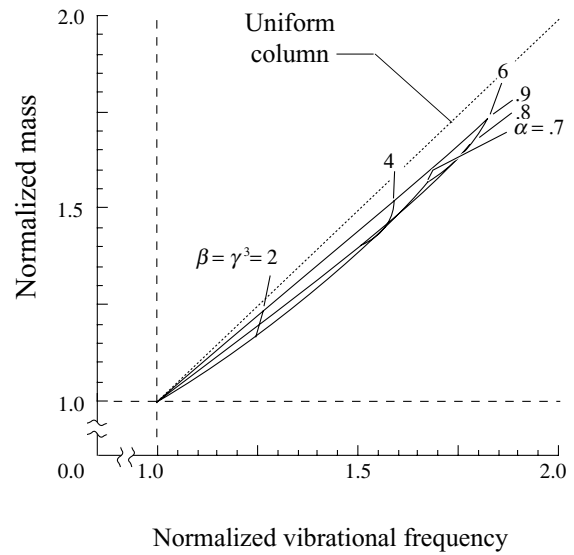
$$\bar{\omega} = \bar{\omega}_o \sqrt{1 - \frac{P}{\bar{P}}} \quad (47)$$

where $\bar{\omega}_o$ is the normalized natural frequency of the column (no axial load), \bar{P} is the normalized buckling load of the column, and $-$ is the normalized axial compressive load in the column.

Although it appears impossible to establish equation (47) analytically for a column with a piecewise constant cross section under axial load, numerical examples should shed some light on the question of its applicability. Table I presents the values of length, bending stiffness, and distributed mass ratios for five selected column configurations along with the numerical solutions for their normalized buckling loads and natural vibration frequencies. The sixth row in table I lists the values selected for the axial load (P/\bar{P}). (Note, negative numbers indicate tension and positive numbers indicate compression.) Finally, the last two rows of table I present the numerical solution for vibration frequency ($(\bar{\omega}/\bar{\omega}_o)_{\text{numerical}}$) and the solution determined from equation (47) ($(\bar{\omega}/\bar{\omega}_o)_{\text{eq. (47)}}$) for each configuration. It can be seen that these solutions agree very well, the differences likely being attributable to numerical inaccuracies.



(a) $0.2 \leq \alpha \leq 0.7$.



(a) $0.7 \leq \alpha \leq 1.0$.

Figure 6 Mass versus vibration frequency where mass is proportional to cube root of bending stiffness.

Figure 7 is a plot of equation (47) superimposed over the data points presented in table I. Although the set of configurations considered is certainly not exhaustive, it represents a reasonable range of the dimensionless parameters. The results strongly suggest that equation (47) indeed predicts the correct vibration frequency for columns with piecewise constant cross sections. If so, then to determine the effect of axial load on vibration frequency in a column of this type, it is necessary only to calculate the buckling load and natural vibration frequency of the column, then apply equation (47) to determine its vibration frequency under axial load.

Table I. Numerical Examples of Column Vibration With Axial Load

Parameter	Configuration				
	1	2	3	4	5
α	0.4	0.4	0.6	0.8	0.8
β	4.0	4.0	2.0	2.0	6.0
γ	4.0	1.5874	1.2599	2.0	1.8171
\bar{P}_{cr}	2.0107	2.0107	1.8123	1.9738	5.5849
$\bar{\omega}_o$	0.8463	1.2354	1.2162	0.9970	1.7673
\bar{P}/\bar{P}	-0.75	-0.5	0.25	0.5	0.75
$(\bar{\omega}/\bar{\omega}_o)_{\text{numerical}}$	1.3167	1.2225	0.8661	0.7050	0.5004
$(\bar{\omega}/\bar{\omega}_o)_{\text{eq. (47)}}$	1.3229	1.2247	0.8660	0.7071	0.5000

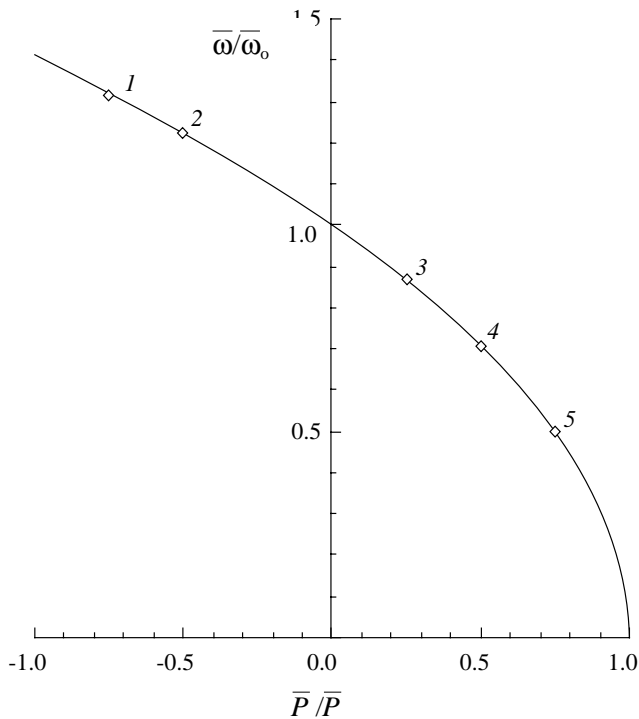


Figure 7. Effect of axial load on fundamental vibration frequency.

Concluding Remarks

The results of an analytical study of the buckling and vibration characteristics of a column with piecewise constant cross section have been presented. Parametric structural efficiency analyses determined that, for increased buckling resistance, the optimum ratio between lengths of the stiffened center section and the entire column is approximately 0.7. Also it was determined that a column using this ratio of lengths offers a mass savings of 6 to 12 percent relative to a uniform column having the same buckling

load. Furthermore, the magnitude of this mass savings was shown to be dependent on the relationship between the bending stiffness and mass per unit length of the column cross section.

Similar parametric structural efficiency analyses were performed using a nondimensionalized set of the governing vibration equations. From these analyses, it was determined that the relationship between bending stiffness and mass per unit length of the column cross section has a great effect on the efficiency of the column from a vibration standpoint. If the mass per unit length and bending stiffness are proportional, a column with a piecewise constant cross section is less efficient than a uniform column, based on fundamental vibration frequency. However, if the mass per unit length is proportional to the cube root of the bending stiffness, a column with a piecewise constant cross section is more efficient than a uniform column, based on either fundamental vibration frequency or buckling load.

Finally, numerical results strongly suggest that the relation between axial load and fundamental vibration frequency for a uniform column also holds for a column with piecewise constant cross section.

NASA Langley Research Center
Hampton, VA 23665-5225
January 31, 1991

References

1. Timoshenko, Stephen P.; and Gere, James M.: *Theory of Elastic Stability*, Second ed. McGraw-Hill Book Co., 1961.
2. Heard, W. L., Jr.; Bush, H. G.; and Agranoff, Nancy: *Buckling Tests of Structural Elements Applicable to Large Erectable Space Trusses*. NASA TM-78628, 1978.
3. Burden, Richard L.; and Faires, J. Douglas: *Numerical Analysis, Third ed.* PWS-KENT Publ. Co., c.1985.
4. Roark, Raymond J.; and Young, Warren C.: *Formulas for Stress and Strain, Fifth ed.* McGraw-Hill Book Co., c.1982.

5. Crandall, Stephen H.: *Engineering Analysis - A Survey of Numerical Procedures*. Robert E. Krieger Publishing Co., c.1986.
6. Timoshenko, S.; Young, D. H.; and Weaver, W., Jr.: *Vibration Problems in Engineering, Fourth ed.* John Wiley & Sons, Inc., c.1974.



Report Documentation Page

1. Report No. NASA TP-3090	2. Government Accession No.	3. Recipient's Catalog No.	
4. Title and Subtitle Buckling and Vibration Analysis of a Simply Supported Column With a Piecewise Constant Cross Section		5. Report Date March 1991	
		6. Performing Organization Code	
7. Author(s) Mark S. Lake and Martin M. Mikulas, Jr.		8. Performing Organization Report No. L-16854	
9. Performing Organization Name and Address NASA Langley Research Center Hampton, VA 23665-5225		10. Work Unit No. 506-43-41-02	
		11. Contract or Grant No.	
12. Sponsoring Agency Name and Address National Aeronautics and Space Administration Washington, DC 20546-0001		13. Type of Report and Period Covered Technical Paper	
		14. Sponsoring Agency Code	
15. Supplementary Notes			
16. Abstract <p>This paper presents an analysis and sample results of the lateral buckling and vibration of a compressively loaded column whose cross section is piecewise constant along its length. The column is symmetric about its midspan and consists of three sections, with the center section having a stiffer cross section than the two identical outboard sections. Buckling and vibration characteristics of the column are determined from a numerical solution of the exact eigenvalue problems. Parametric structural efficiency analyses are performed using a nondimensionalized set of governing equations to determine the optimum ratio between the lengths of the center section and the outboard sections based on both buckling load and vibration frequency requirements. In these analyses two relationships between cross-sectional mass and bending stiffness are considered; one is a low-efficiency method for increasing the bending stiffness of the cross section, and the other is a high-efficiency method. The effect of axial load on vibration frequency is also examined and compared with that of a uniform column.</p>			
17. Key Words (Suggested by Author(s)) Tapered column Buckling Stability Vibration Beam-column Truss structure		18. Distribution Statement Unclassified-Unlimited <div style="text-align: right;">Subject Category 39</div>	
19. Security Classif. (of this report) Unclassified	20. Security Classif. (of this page) Unclassified	21. No. of Pages 11	22. Price A03